

Do $\Xi\Xi$ bound states exist?

J. Haidenbauer¹, Ulf-G. Meißner^{2,1}, and S. Petschauer³

¹*Institute for Advanced Simulation and Jülich Center for Hadron Physics,
Institut für Kernphysik, Forschungszentrum Jülich, D-52425 Jülich, Germany*

²*Helmholtz-Institut für Strahlen- und Kernphysik and Bethe Center
for Theoretical Physics, Universität Bonn, D-53115 Bonn, Germany*

³*Physik Department, Technische Universität München, D-85747 Garching, Germany*

The existence of baryon-baryon bound states in the strangeness sector is examined in the framework of SU(3) chiral effective field theory. Specifically, the role of SU(3) symmetry breaking contact terms that arise at next-to-leading order in the employed Weinberg power counting scheme is explored. We focus on the 1S_0 partial wave and on baryon-baryon channels with maximal isospin since in this case there are only two independent SU(3) symmetry breaking contact terms. At the same time, those are the channels where most of the bound states have been predicted in the past. Utilizing pp phase shifts and Σ^+p cross section data allows us to pin down one of the SU(3) symmetry breaking contact terms and a clear indication for the decrease of attraction when going from the NN system to strangeness $S = -2$ is found, which rules out a bound state for $\Sigma\Sigma$ with isospin $I = 2$. Assuming that the trend observed for $S = 0$ to $S = -2$ is not reversed when going to $\Xi\Sigma$ and $\Xi\Xi$ makes also bound states in those systems rather unlikely.

PACS numbers: 13.75.Ev, 14.20.Jn, 12.39.Fe, 25.80.Pw

Keywords: Baryon-baryon interactions, chiral effective field theory

I. INTRODUCTION

Dibaryons (as compact six-quark systems or as bound states formed by two conventional octet and/or decuplet baryons) have been intriguing objects of investigations and speculations for many years. While in the purely nucleonic case there is yet again a promising dibaryon candidate [1], besides the deuteron, there are indications that the strangeness sector could be specifically rewarding for finding dibaryons [2]. Here the by far best-known example is certainly the H -dibaryon suggested by Jaffe [3], a deeply bound state with quantum numbers of the $\Lambda\Lambda$ system, i.e. strangeness $S = -2$ and isospin $I = 0$, and with $J^P = 0^+$. There are also speculations about the existence of other exotic states, notably in the $S = -3$ ($N\Omega$) [4, 5] and $S = -6$ ($\Omega\Omega$) [6, 7] systems, see also Refs. [8, 9].

With regard to two octet baryons, the (approximate) SU(3) flavor symmetry of the strong interaction suggests that bound states could exist for systems with strangeness $S = -3$ and, in particular, $S = -4$ [10]. Indeed, meson-exchange models like the Nijmegen baryon-baryon (BB) interaction [11, 12], derived under the assumption of (broken) SU(3) symmetry, predict interactions for the $S = -3$ and -4 sectors that are fairly strong and attractive and lead to bound states in the $\Xi\Sigma$ and $\Xi\Xi$ channels [13, 14]. The situation is somewhat different for BB interactions derived in the constituent quark model by Fujiwara and collaborators [15]. While SU(3) flavor symmetry plays likewise a key role in extending the model from the NN and YN interaction (where free parameters are fixed) to the $S = -3$ and -4 channels, in this approach it was found that the BB interaction becomes step by step less attractive when going from strangeness $S = 0$ to $S = -4$. In particular,

no dibaryon bound states are supported, except for the deuteron. A similar pattern was reported in Ref. [16] where the intermediate-range attraction from the scalar-isoscalar (“ σ ”) channel was evaluated within a model for correlated $\pi\pi$ and $\bar{K}K$ exchange between octet baryons. Also in this case it was found that the attraction between two baryons, quantified by the effective σ -meson coupling strength, decreases step by step in the strangeness sector.

Results obtained in lattice QCD calculations are conflicting so far. While a $\Xi\Xi$ bound state was found by the NPLQCD collaboration [17] (in the 1S_0 state), the HAL QCD collaboration reported only a moderately attractive interaction for that partial wave [18].

In the present paper we examine the existence of $\Sigma\Sigma$, $\Xi\Sigma$ and $\Xi\Xi$ bound states in the framework of SU(3) chiral effective field theory (EFT). In particular, we explore the role of SU(3) symmetry breaking contact terms that arise at next-to-leading order (NLO) in the perturbative expansion of the baryon-baryon potential. A first study of the baryon-baryon (BB) interactions within chiral EFT [19] in the Weinberg scheme [20, 21] for the strangeness $S = -2$, -3 and -4 sectors was presented in Refs. [22, 23]. At leading-order (LO) considered in those works the chiral potentials consist of contact terms without derivatives and of one-pseudoscalar-meson exchanges (π , K , η). Assuming SU(3) flavor symmetry those contact terms and the couplings of the pseudoscalar mesons to the baryons can be related to the corresponding quantities of the $S = -1$ hyperon-nucleon (YN) channels. Specifically, the values of the pertinent five low-energy constants (LECs) related to the contact terms could be fixed from the study of the ΛN and ΣN systems [19] and then genuine predictions for the $\Xi\Lambda$, $\Xi\Sigma$, and $\Xi\Xi$ interactions could be made at LO. Strong attraction was found in some of the $S = -2$, -3 and -4 BB channels, and

several bound states were predicted [23].

Recently, a YN interaction has been derived up to NLO in chiral EFT by the Jülich-Bonn-Munich group [24]. At that order contact terms leading to an explicit SU(3) symmetry breaking appear for the first time [24, 25] as mentioned above. Since the sparse experimental information on ΛN and ΣN scattering could be described rather well with using the SU(3) symmetric terms alone, SU(3) symmetry breaking was simply neglected. In other words it was assumed that the LECs associated with those contact terms are zero. Thus, in the actual calculation the SU(3) symmetry is only broken via the employed physical masses of the involved mesons and octet baryons (N , Λ , Σ , Ξ).

On the other hand, it was also found in Ref. [24] that a simultaneous description of the YN data and the nucleon-nucleon (NN) phase shifts is not possible on the basis of SU(3) symmetric contact terms. In particular, the strengths needed for reproducing the pp (or np) 1S_0 phase shifts and the Σ^+p cross section could not be reconciled in a scenario which maintained SU(3) symmetry for the contact terms. This observation is the starting point for the present study, because it can be used to put constraints on the SU(3) symmetry breaking contact terms. In particular, the situation in the 1S_0 partial wave and for BB channels with maximal isospin is rather simple and interesting. Here, there are only two independent SU(3) symmetry breaking LECs at NLO for five physical channels, and for three of those five channels bound states have been predicted in the past. The aforementioned pp phase shifts and the Σ^+p cross section allow us to pin down one of the symmetry breaking LECs and provide a clear-cut indication for the decrease of attraction when one goes from the NN system to $S = -2$, so that a bound state for $\Sigma\Sigma$ with isospin $I = 2$ can be practically ruled out. The other LEC cannot be determined at present and several options for its value are discussed. However, already the assumption that the trend one sees for $S = 0$ to $S = -2$ is not reversed when going to $S = -3$ and $S = -4$ makes bound states in the latter systems rather unlikely.

The paper is structured in the following way: In Sect. 2 we provide a basic introduction to our BB interaction derived in chiral EFT. We also discuss the changes that arise in the interaction when the SU(3) symmetry breaking contact terms are taken into account. Selected results for BB systems with strangeness $S = -2$ to $S = -4$ based on SU(3) symmetric contact terms fixed in a fit to YN data are presented in Sect. 3. In Sect. 4 we introduce the SU(3) symmetry breaking contact terms and show the implications for the 1S_0 phase shift in the $\Sigma\Sigma$, $\Xi\Sigma$, and $\Xi\Xi$ channels with maximal isospin. The paper ends with a short summary. Some technical information about our calculation is given in Appendix A.

II. THE BARYON-BARYON INTERACTION IN CHIRAL EFT

A comprehensive description of the derivation of the chiral BB potentials for the strangeness sector using the Weinberg power counting can be found in Refs. [19, 24–26]. The LO potential consists of four-baryon contact terms without derivatives and of one-pseudoscalar-meson exchanges while at NLO contact terms with two derivatives arise, together with contributions from (irreducible) two-pseudoscalar-meson exchanges. The interaction in Ref. [24] was derived by imposing SU(3) flavor symmetry. Then the contributions from pseudoscalar-meson exchanges (π , η , K) are completely fixed in terms of the axial coupling g_A and α , the so-called $F/(F + D)$ ratio, together with the pion decay constant f_0 .

SU(3) symmetry was also imposed for the contact terms. Since the strength parameters associated with the contact terms, the LECs, need to be determined by a fit to data, it was tried to keep the number of independent LECs that can contribute as small as possible. In the SU(3) symmetric case there are in total 13 LECs entering the S -waves and the S - D transitions of the ΛN - ΣN system [24], and their values could be fairly well fixed in a fit to the available low-energy total cross sections for $\Lambda p \rightarrow \Lambda p$, $\Sigma^- p \rightarrow \Lambda n$, $\Sigma^- p \rightarrow \Sigma^0 n$, $\Sigma^- p \rightarrow \Sigma^- p$, and $\Sigma^+ p \rightarrow \Sigma^+ p$. However, it would have been not possible to determine the additional 5 contact terms appearing at NLO that lead to an explicit SU(3) symmetry breaking, cf. the Appendix of Ref. [24] and also Ref. [25], and, therefore, the corresponding LECs were simply set to zero.

At the same time, it became already clear in Ref. [24] that it is impossible to obtain a combined fit to the YN data and to the NN phase shifts with LECs that fulfill SU(3) symmetry. The most obvious case is the 1S_0 partial wave, where SU(3) symmetry implies that the interactions in the NN ($I=1$) and ΣN ($I=3/2$) channels involve the very same two LECs and are given simply by

$$V(^1S_0) = \tilde{C}_{iS_0}^{27} + C_{iS_0}^{27}(p^2 + p'^2), \quad (1)$$

with p and p' being the center-of-mass momenta in the initial and final state. The label $\{27\}$ indicates that both channels belong to the $\{27\}$ representation of SU(3) [27, 28], see Ref. [24] for a detailed description of the notation. Indeed, strict SU(3) symmetry suggests that the 1S_0 contact interaction should be the same for several BB channels that belong solely to the $\{27\}$:

$$V_{NN}^{(I=1)} = V_{\Sigma N}^{(I=3/2)} = V_{\Sigma\Sigma}^{(I=2)} = V_{\Xi\Sigma}^{(I=3/2)} = V_{\Xi\Xi}^{(I=1)}. \quad (2)$$

Eq. (1) implies that under the assumption of SU(3) symmetry the (hadronic part of the) interaction in the $\Sigma^- n$ or $\Sigma^+ p$ channels is unambiguously fixed once the LECs are determined from the np or pp phases, or vice versa. In practice it turned out that with LECs fixed from the np (or pp) phase shifts a near-threshold bound state is generated in the $\Sigma^+ p$ system and, as a consequence, the

empirical Σ^+p cross section is grossly overestimated [24]. Evidently, SU(3) symmetry breaking in the contact terms has to be taken into account if one wants to describe NN and ΣN scattering simultaneously.

The contact terms, including the SU(3) symmetry breaking corrections that arise at NLO, have been worked out explicitly in Ref. [25] for all octet BB channels from strangeness $S = 0$ to -4 . There are twelve independent SU(3) symmetry breaking LECs in total, see Ref. [25], of which six occur in the 1S_0 partial wave and the other six in the 3S_1 . It is impossible to determine all of those based on the presently available experimental information in the strangeness $S = -1$ to -4 sectors.

The situation is more favorable, however, in the particular case discussed above, namely for the 1S_0 partial wave and BB channels with maximal isospin. Here one obtains

$$\begin{aligned} V_{NN}^{(I=1)} &= \tilde{C}_{1S_0}^{27} + C_{1S_0}^{27}(p^2 + p'^2) + \frac{1}{2}C_1^\chi(m_K^2 - m_\pi^2), \\ V_{\Sigma N}^{(I=3/2)} &= \tilde{C}_{1S_0}^{27} + C_{1S_0}^{27}(p^2 + p'^2) + \frac{1}{4}C_1^\chi(m_K^2 - m_\pi^2), \\ V_{\Sigma\Sigma}^{(I=2)} &= \tilde{C}_{1S_0}^{27} + C_{1S_0}^{27}(p^2 + p'^2), \\ V_{\Xi\Sigma}^{(I=3/2)} &= \tilde{C}_{1S_0}^{27} + C_{1S_0}^{27}(p^2 + p'^2) + \frac{1}{4}C_2^\chi(m_K^2 - m_\pi^2), \\ V_{\Xi\Xi}^{(I=1)} &= \tilde{C}_{1S_0}^{27} + C_{1S_0}^{27}(p^2 + p'^2) + \frac{1}{2}C_2^\chi(m_K^2 - m_\pi^2). \end{aligned} \quad (3)$$

Evidently, there are only two additional LECs due to SU(3) symmetry breaking, which are denoted by C_1^χ and C_2^χ in the above equations. As expected, their contributions are proportional to the meson mass difference, $m_K^2 - m_\pi^2$, so that they vanish in case of SU(3) symmetry, i.e. when $m_K^2 \equiv m_\pi^2$. There are also contact terms proportional to m_π^2 and m_K^2 which are, however, SU(3) symmetric and have been absorbed into the definition of $\tilde{C}_{1S_0}^{27}$ [25]. A combined fit to the pp (or np) 1S_0 phase shifts and the Σ^+p cross section allows us to determine three of the four LECs in Eq. (3), as will be demonstrated below. Then we can make genuine predictions for the $\Sigma\Sigma$ interaction with isospin $I = 2$. The fourth LEC (C_2^χ) cannot be pinned down reliably at present. In this case we will consider a range of values and study the consequences for the possible existence of $\Xi\Sigma$ and $\Xi\Xi$ bound states.

For completeness let us mention that our calculations are done in momentum space. We solve the partial-wave projected (non-relativistic) Lippmann-Schwinger (LS) equation,

$$T_{B_1 B_2}(p'', p'; \sqrt{s}) = V_{B_1 B_2}(p'', p') + \int_0^\infty \frac{dp p^2}{(2\pi)^3} V_{B_1 B_2}(p'', p) \frac{2\mu_{B_1 B_2}}{k^2 - p^2 + i\epsilon} T_{B_1 B_2}(p, p'; \sqrt{s}) \quad (4)$$

for a particular BB channel. Here, $\mu_{B_1 B_2}$ is the reduced mass and k is the on-shell momentum, which is defined by $\sqrt{s} = \sqrt{M_{B_1}^2 + k^2} + \sqrt{M_{B_2}^2 + k^2}$. Relativistic kinematics is used for relating the laboratory momentum p_{lab} of the baryons to the center-of-mass momentum. In case of pp and Σ^+p , where we compare with experiments, the Coulomb interaction is included. This is done via the Vincent-Phatak method [29]. The potentials in the LS equation are cut off with a regulator function, $f_R(\Lambda) = \exp[-(p'^4 + p^4)/\Lambda^4]$, in order to remove high-energy components [30]. In Ref. [24] results for cutoff values in the range $\Lambda = 500 - 650$ MeV were shown and we will consider the same range here. The variation of the results with the cutoff can be viewed as a rough estimate for the theoretical uncertainty [30]. A better method to determine the theoretical uncertainty has recently been proposed for the NN sector [31], but in view of the scarce data in the strangeness sector and given the exploratory character of our study, we stick to the much simpler procedure of varying the cutoff.

Note that for all the systems listed in Eq. (3) there is no coupling to other partial waves or channels. Thus,

differences in the reaction thresholds that generate an additional SU(3) symmetry breaking in the scattering amplitude when the LS equation (4) is solved for coupled channels, are absent. This makes those systems especially suited for isolating SU(3) symmetry breaking effects in the potential.

III. RESULTS BASED ON THE LOW ENERGY CONSTANTS OF OUR NLO YN POTENTIAL

In this section we present predictions for the $\Sigma\Sigma$, $\Xi\Sigma$ and $\Xi\Xi$ channels, where SU(3) symmetry is assumed for the contact terms. To be exact, SU(3) symmetry is utilized to relate the LECs for the $S = -2, -3$ and -4 systems to those determined in the fit to the ΛN and ΣN data [24]. The symmetry is broken by the used physical masses of the involved mesons and baryons. Note that the meson masses induce an explicit symmetry breaking into the BB potential while the baryon masses enter only in the course of solving the scattering equation, because they appear in the integral equation in form of the re-

TABLE I. $\Sigma\Sigma$, $\Xi\Sigma$ and $\Xi\Xi$ scattering lengths (in fm) in the 1S_0 partial wave. Results are given for our LO [19] and NLO [24] interactions based on LECs fitted to the YN data. For comparison some values for the Nijmegen NSC97 potential [13] and a quark model [15] are also included.

	χ EFT LO	χ EFT NLO	NSC97a [13]	NSC97f [13]	fss2 [15]
Λ [MeV]	550 \cdots 700	500 \cdots 650			
$a_{\Sigma\Sigma}^{I=2}$	-6.2 \cdots -9.3	60.6 \cdots -286.0	10.32	6.98	-85.3
$a_{\Xi\Lambda}$	-33.5 \cdots 9.07	-7.4 \cdots -13.5	-0.80	-2.11	-1.08
$a_{\Xi\Sigma}^{I=3/2}$	4.28 \cdots 2.74	8.4 \cdots 13.8	4.13	2.32	-4.63
$a_{\Xi\Xi}^{I=1}$	3.92 \cdots 2.47	9.7 \cdots 6.5	17.81	2.38	-1.43

duced mass, see Eq. (4).

In a corresponding investigation with our LO potential it was found that the interaction in some of the $S = -3$ and -4 channels is strongly attractive and even bound states were predicted [22, 23]. The same happens also at NLO as one can see from the results for the 1S_0 partial wave summarized in Tables I and II. Specifically, in all channels where large scattering lengths were found at LO, they are likewise large at NLO. And, except for $\Xi\Lambda$, the scattering lengths are large and positive – a clear indication for bound states. In case of $\Sigma\Sigma$ the NLO interaction produces a pole very close to the threshold which, depending on the cutoff, corresponds either to a bound state (large positive scattering length) or to a virtual state (large negative scattering length). The actual binding energies of those states are listed in Table II. Comparing the NLO results with the ones at LO one notices that the $\Xi\Xi$ and $\Xi\Sigma$ binding energies have become somewhat smaller. Indeed in both cases the systems are now only fairly weakly bound. We do not include the Coulomb interaction in the calculation of the strangeness $S = -2$ to -4 sectors. (For bound states this would be technically rather complicated within the Vincent-Phatak method employed by us.) It is quite possible that the additional repulsion due to the Coulomb force could even make the $\Sigma\Sigma$ system unbound. In this context we want to point out that it is good to see that the cutoff dependence of the binding energies is strongly reduced at NLO.

Table I contains also the scattering lengths predicted by the Nijmegen NSC97 meson-exchange model [11] and of a BB potential by Fujiwara and collaborators [15] derived in the quark model. The Nijmegen interaction suggests bound states in the $\Sigma\Sigma$, $\Xi\Sigma$ and $\Xi\Xi$ channels, as can be guessed from the large and positive scattering length. The latest version of the Nijmegen potential [12] produces a bound state in the $\Xi\Xi$ channel [14] too. As already mentioned in the Introduction, no bound states were found for the quark-model interaction [15], though the $\Sigma\Sigma$ interaction is seemingly very close to producing a bound state as indicated by the large negative scattering length.

TABLE II. Binding energies of various BB bound states (in MeV) in the 1S_0 partial wave, for our LO [19] and NLO [24] interactions based on LECs fitted to the YN data.

	χ EFT LO	χ EFT NLO
Λ [MeV]	550 \cdots 700	500 \cdots 650
$\Sigma\Sigma$ ($I = 2$)	–	0 \cdots -0.01
$\Xi\Sigma$ ($I = 3/2$)	-2.23 \cdots -6.18	-0.58 \cdots -0.19
$\Xi\Xi$ ($I = 1$)	-2.56 \cdots -7.27	-0.40 \cdots -1.00

IV. RESULTS WITH INCLUSION OF SU(3) SYMMETRY BREAKING CONTACT TERMS

For studying the effects of SU(3) symmetry breaking we performed fits to NN and YN data, requiring that C^{27} is the same in line with the power counting where (SU(3) symmetry breaking) corrections to \tilde{C}^{27} arise at NLO but not to C^{27} . With regard to NN the fit was performed to the 1S_0 pp phase shifts of the GWU analysis [32, 33]. Since the pp interaction is slightly less attractive than the one in np , cf. the scattering lengths of ≈ -17 fm (for the purely hadronic pp interaction) versus -23.75 fm, the amount of SU(3) symmetry breaking we need to introduce is also somewhat smaller. The LEC C^{27} was determined in the pp sector and then taken over in the subsequent calculations in the strangeness sector. It turned out that the actual value of C^{27} found in the fits depends only very weakly on the cutoff mass and, therefore, we adopted a single value for all cutoffs.

The Σ^+p interaction was fitted to the corresponding 1S_0 phase shift predicted by our chiral EFT YN interaction [24]. We could not simply take over the results of Ref. [24] because that interaction is based on a single decay constant $f_0 \approx f_\pi \approx 93$ MeV. Now we want to take into account also the experimentally known differences between f_π , f_η , and f_K in the evaluation of the pertinent coupling constants. In the fit we made sure that there is perfect agreement with the results of [24] in the (low-energy) region where Σ^+p cross section data are available. In fact, for one cutoff ($\Lambda = 600$ MeV) we even performed a full fit to all YN data considered in [24] in order to check whether the same χ^2 can be achieved –

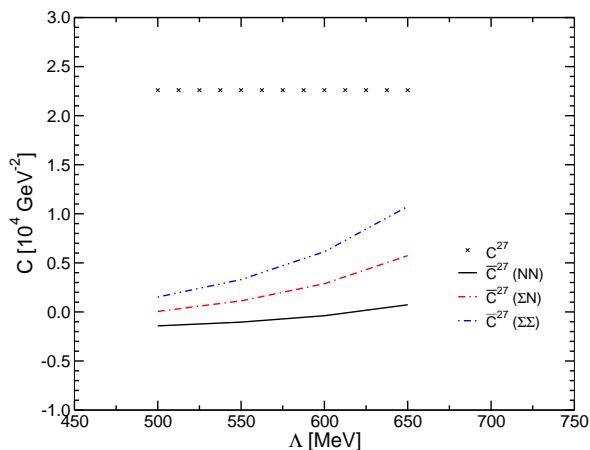


FIG. 1. Low-energy constants employed in the different BB channels, for the considered cutoff values Λ . Here $\bar{C}^{27}(NN) = \tilde{C}^{27} + \frac{1}{2}C_1^X(m_K^2 - m_\pi^2)$, etc., see Eq. (3). C^{27} is in units of 10^4 GeV^{-4} .

which was indeed the case.

It turns out that $C_1^X < 0$, i.e. one needs more repulsion to fit Σ^+p (YN) data than to fit the pp 1S_0 phase shift. The LECs are graphically presented in Fig. 1, while the phase shifts are shown in Fig. 2. For the former we show the sum of the LO contact term \tilde{C}^{27} and the SU(3) symmetry breaking contribution for each BB channel, e.g. $\bar{C}^{27} = \tilde{C}^{27} + \frac{1}{2}C_1^X(m_K^2 - m_\pi^2)$ for the NN system, so that one can see how the repulsion effectively increases when going from $S = 0$ to -2 . The values of the employed LECs are summarized in Table III.

TABLE III. Employed low energy constants for various cut-offs. The values for \tilde{C}^{27} are in 10^4 GeV^{-2} , those for C^{27} and C_1^X in 10^4 GeV^{-4} .

Λ (MeV)	\tilde{C}^{27}	C^{27}	C_1^X
500	0.15196	2.26	-2.6014
550	0.32963	2.26	-3.8346
600	0.61394	2.26	-5.7731
650	1.0752	2.26	-8.8719

The experimental Σ^+p cross section provides an upper limit on the phase shift for the Σ^+p 1S_0 partial wave. The limit can be derived from the expression for the partial cross section,

$$\sigma_{\Sigma^+p; J} = \frac{(2J+1)\pi}{k^2} \sin^2 \delta_J, \quad (5)$$

J being the total angular momentum, by assuming that the 1S_0 contribution alone already saturates the cross section data. Pertinent results are included in Fig. 2, see the filled circles. Obviously for our EFT interaction [24] (but also for most of the YN potentials based on meson

exchange [11, 12, 34, 35]) the predicted 1S_0 amplitude is very close to saturating the Σ^+p cross section alone. The hatched band in Fig. 2 indicates the predictions one would get for the Σ^+p channel with the LECs fitted to the pp 1S_0 phase shifts. Evidently, the assumption of SU(3) symmetry for the contact terms is in clear contradiction with the experimental information.

Note that there is also a phase shift analysis for Σ^+p [36] at a single momentum, namely $p_{lab} = 170 \text{ MeV}/c$, which suggests a value of around 26 degrees for the 1S_0 partial wave. However, that analysis is not model independent and, therefore, we have more confidence in our own results determined by a fit to existing YN data within chiral EFT.

Once we have determined \tilde{C}^{27} , C^{27} , and C_1^X from our fit to the pp and Σ^+p 1S_0 phase shifts, we can make predictions for the $\Sigma\Sigma$ case, see Eq. (3). Corresponding results are shown in Fig. 3. The phase shifts attest that there is a sizable attraction in this channel but the actual values are in the order of 30 degrees and, thus, far away from the SU(3) symmetric case discussed in Sect. 2 where the $\Sigma\Sigma$ system with $I = 2$ was more or less bound. In particular, the predicted scattering lengths are now around -3.2 to -3.4 fm only. Indeed, the present result at NLO that follows directly from the SU(3) symmetry breaking observed between pp and Σ^+p practically rules out a bound state in this channel.

The actual value of C_2^X can be only determined by a fit to pertinent (ΞY and/or $\Xi\Xi$) data. Since such data are not available, in the following let us consider some exemplary choices for C_2^X . In particular, we presume that the magnitude of the SU(3) breaking LEC C_2^X is comparable to C_1^X and that the trend in the SU(3) symmetry breaking we see for $NN \Rightarrow \Sigma N \Rightarrow \Sigma\Sigma$, is not reversed for the $S = -3$ and -4 systems. The latter means that we suppose C_2^X to be positive, based on its definition via Eq. (3). A simple assumption is $C_2^X \approx 0$, so that there is no further SU(3) symmetry breaking in the contact terms beyond $S = -2$. The other extreme consists in assuming that $C_2^X \approx -C_1^X$, which implies that the same SU(3) symmetry breaking required to describe pp and Σ^+p occurs also between the $S = -2$, -3 , and -4 BB systems. Finally, we consider an intermediate case, namely $C_2^X \approx -C_1^X/2$.

Predictions for the $\Xi\Sigma$ ($I = 3/2$) and $\Xi\Xi$ ($I = 1$) 1S_0 phase shifts resulting from the three choices are presented in Fig. 4. In the case $C_2^X \approx 0$ (hatched band) the only SU(3) symmetry breaking effects in the potential (as compared to $\Sigma\Sigma$) come from the one- and two-meson exchange contributions. One notices a clear increase in the attraction for $\Xi\Sigma$ and $\Xi\Xi$ in comparison to the $\Sigma\Sigma$ results, cf. Fig. 3 with Fig. 4. Specifically, for $\Xi\Xi$ the phase shifts reach almost 60 degrees, i.e. similar values as in the pp system. Introducing an explicit SU(3) symmetry breaking in the contact terms leads to the results represented by the filled bands ($C_2^X \approx -C_1^X/2$) and dotted bands ($C_2^X \approx -C_1^X$), respectively. Now the predicted phase shifts for the 1S_0 partial wave are much smaller and especially in the $\Xi\Xi$ case the reduction is drastic.

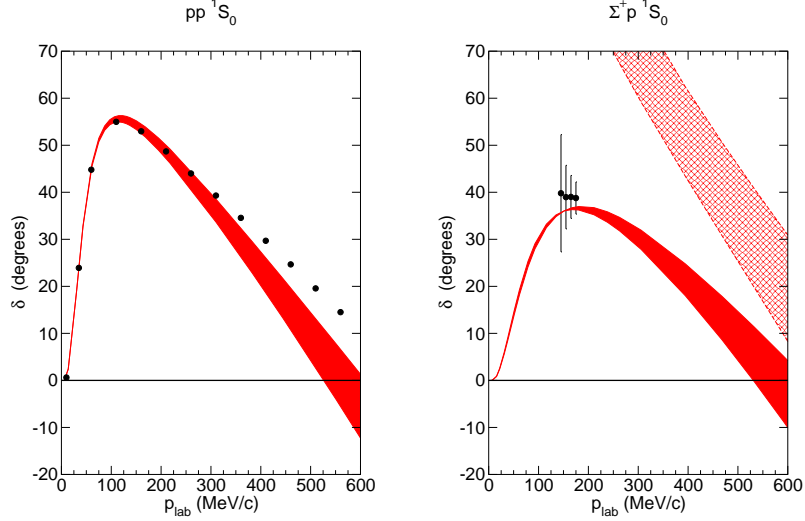


FIG. 2. pp and Σ^+p phase shifts in the 1S_0 partial wave. The filled band represent our results at NLO. The hatched band shows Σ^+p result based on LECs fixed by a fit to pp phase shifts. The pp phase shifts of the GWU analysis [33] are shown by circles. In case of Σ^+p the circles indicate upper limits for the phase shifts, deduced from the Σ^+p cross section, see text.

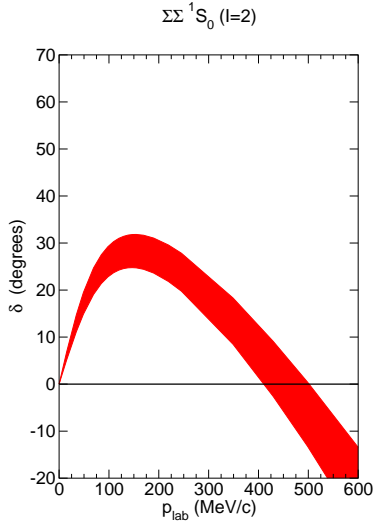


FIG. 3. Phase shifts for the 1S_0 partial wave in the $\Sigma\Sigma$ channel with isospin $I = 2$. The band is our prediction based on the LECs \bar{C}^{27} and C^{27} fixed from a fit to pp and Σ^+p , see Eq. (3).

The scattering length for the $\Xi\Sigma$ channel are in the range of -3.7 to -2.8 fm for the choice $C_2^X \approx 0$, but reduce to -1.3 to -1.8 fm for $C_2^X \approx -C_1^X/2$, and to -0.7 to -1.0 fm for $C_2^X \approx -C_1^X$. For $\Xi\Xi$ we obtain -7.0 to

-13.5 fm, -1.6 to -1.8 fm, and ≈ 0.7 fm, respectively.

We have also performed calculations based on the np 1S_0 phase shifts as starting point instead of the pp values. In this case there is a somewhat stronger SU(3) symmetry breaking between np and Σ^+p and, accordingly, the resulting $\Sigma\Sigma$, $\Xi\Sigma$ and $\Xi\Xi$ phase shifts are then reduced by roughly 10 % as compared to the ones presented in Figs. 2, 3 and 4.

There are results for the $\Xi\Xi$ 1S_0 partial wave from lattice QCD calculations. The ones reported by the NPLQCD collaboration [17] suggest a bound state with $E_B = -14.0 \pm 1.4 \pm 6.7$ MeV. The calculation was performed for a pion mass of $m_\pi = 389$ MeV and for $M_\Xi = 1349.6$ MeV. In contrast, no bound state was found by the HAL QCD collaboration [18]. In this calculation, that corresponds to $m_\pi = 510$ MeV and $M_\Xi = 1456$ MeV, the interaction in the 1S_0 partial wave is only moderately attractive and the phase shifts rise only to a maximum of around 20 ± 10 degrees. Interestingly, the EFT predictions based on the choice $C_2^X \approx -C_1^X/2$ are fairly close to those results. Our investigations in Refs. [37, 38] suggest that the actual value of the pion mass does not play an important role in the $\Xi\Xi$ system and, therefore, we do not expect sizable changes in the lattice results once calculations for masses closer to the physical value become feasible. The Ξ mass is only marginally larger than the physical mass (which is about 1320 MeV) in case of the NPLQCD collaboration so that it should not distort the results. In any case, a smaller baryon mass would rather lead to a reduction of the attraction than to an enhancement, cf. the discussion below.

Finally, let us comment on the role played by the SU(3)

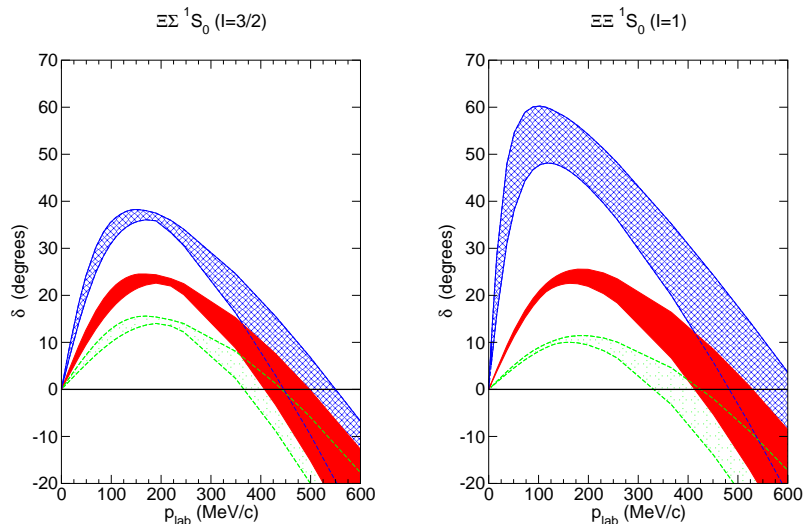


FIG. 4. Phase shifts for the 1S_0 partial wave in the $\Xi\Sigma$ ($I = 3/2$) and $\Xi\Xi$ ($I = 1$) channels. The hatched bands, filled bands, and dotted bands correspond to the choices $C_2^X = 0$, $-C_1^X/2$, and $-C_1^X$, respectively.

symmetry breaking in the baryon masses. As mentioned in Sect. 2, the baryon masses enter solely in the course of solving the LS equation (4). Contributions to the potential involving the baryon masses occur only at higher order in the employed power counting scheme [20, 21, 30]. In fact, this appearance of the reduced BB mass in the LS equation is the key point in the argument exploited by Miller [10] in his exploration of possible $\Xi\Xi$ bound states. His argument is easy to understand in terms of the Schrödinger equation,

$$-\frac{d^2u}{dr^2} + 2\mu_{B_1B_2}V_{B_1B_2}u = k^2u$$

where $u(r)$ is the wave function. If SU(3) symmetry is approximately fulfilled then $V_{NN} \approx V_{\Xi\Xi}$. However, since the physical mass of Ξ is significantly larger than the one of the nucleon, the effective strength of the interaction is increased when it is multiplied with the appropriate reduced mass $\mu_{B_1B_2}$. For example, for $\Xi\Xi$ one has $\mu_{\Xi\Xi}/\mu_{NN} \approx 1.40$, i.e. there is a 40 % increase in the effective strength of the interaction as compared to NN , while for $\Sigma\Sigma$ one gets $\mu_{\Sigma\Sigma}/\mu_{NN} \approx 1.27$. For attractive potentials this has a drastic effect and leads to bound states with increasing baryon masses as demonstrated in the work of Miller for simple potential models. Clearly, the same mechanism is also responsible for the $\Xi\Xi$, etc. bound states that one observes in meson-exchange potentials and in our EFT interactions when SU(3) symmetry is assumed in extrapolating to the strangeness $S = -3$ and -4 BB systems. Indeed, the increase in the phase shift from $\Sigma\Sigma$ (Fig. 3) to $\Xi\Xi$ (Fig. 4) in the scenario with $C_2^X \approx 0$ reported above is primarily dictated by the increase in the corresponding reduced masses.

The actual pp and Σ^+p phase shifts suggest that there is no such net increase in the attraction when going to the strangeness sector. Thus, in practice the SU(3) symmetry breaking LEC C_1^X (more than) compensates effectively the impact of the increase in the reduced mass. Indeed, the stepwise modification of the contact interaction due to the SU(3) symmetry breaking terms that follows from chiral EFT, cf. Eq. (3), is paralleled by a similar stepwise increase in the reduced mass when going from NN to ΣN to $\Sigma\Sigma$, say. Thus, since the mass splitting between Σ and Ξ is significantly smaller than the one between nucleon and Σ , $M_\Xi - M_\Sigma \approx 125$ MeV versus $M_\Sigma - M_N \approx 254$ MeV, one could speculate that the magnitude of the “compensating” SU(3) symmetry breaking LEC (C_2^X) is likewise reduced. If that is so, adopting $C_2^X \approx -C_1^X/2$ might be a reasonable choice. In any case, we believe that a realistical estimation for C_2^X might be provided by $-C_1^X/2 \geq C_2^X \geq 0$. But it is obvious from our results that for any value $C_2^X \geq 0$ the bound states that we find in the $\Sigma\Sigma$, $\Xi\Sigma$ and $\Xi\Xi$ systems for interactions with SU(3) symmetric contact terms (cf. the results presented in Sect. 3) disappear.

V. SUMMARY

In the present paper we examined the question whether baryon-baryon bound states in the strangeness sector could exist in the framework of chiral effective field theory. In particular, we explored the role of SU(3) symmetry breaking contact terms that arise at next-to-leading order in the perturbative expansion in the employed Weinberg scheme. We focused on the 1S_0 partial wave

and on baryon-baryon channels with maximal isospin because in this case there are only two independent SU(3) symmetry breaking contact terms and, at the same time, those are the channels where most of the bound states have been predicted in the past. Utilizing pp phase shifts and Σ^+p cross section data allowed us to pin down one of the SU(3) symmetry breaking contact terms and a clear indication for the decrease of attraction when going from the NN system to strangeness $S = -2$ is found, which practically rules out a bound state for the $\Sigma\Sigma$ 1S_0 partial wave with isospin $I = 2$. Furthermore, if that trend observed for $S = 0$ to $S = -2$ is not reversed when going to the corresponding $\Xi\Sigma$ and $\Xi\Xi$ channels, which we assumed in the present investigation, then also bound states in the latter systems are rather unlikely.

Experiments for BB systems with $S = -3$ or -4 are certainly rather challenging. However, it should be feasible to perform $\Xi\Sigma$ and $\Xi\Xi$ correlations measurements in heavy-ion collisions at RHIC or at CERN, similar to those for $\Lambda\Lambda$ reported recently [39]. From such data conclusions on the strength of the interaction in those systems could be drawn and possibly even on the existence of dibaryons. BB systems with strangeness $S = -2$ to -4 could be also produced in photon induced reactions on the deuteron at JLab as suggested in Ref. [10], or in corresponding K^- induced reactions at J-PARC [40]. As discussed in [41], from such data one could even deduce the scattering lengths for specific BB channels which would then provide a clear signal for the presence (or absence) of bound states. First and foremost, however, it would be good to resolve the discrepancies in the present lattice QCD calculations for the $\Xi\Xi$ system. Hopefully, this can be done soon, because then we could get already a unique and definite answer.

ACKNOWLEDGEMENTS

This work is supported in part by the DFG and the NSFC through funds provided to the Sino-German CRC 110 “Symmetries and the Emergence of Structure in QCD” and by the EU Integrated Infrastructure Initiative HadronPhysics3.

Appendix A: Two-pseudoscalar-meson exchange contributions

The spin-momentum part of the interaction in the $\Sigma\Sigma$, $\Xi\Sigma$ and $\Xi\Xi$ channels is the same as in the YN case and is

described in detail in the Appendix A of Ref. [24]. There are, however, some changes in the isospin coefficients for $\Xi\Sigma$ as compared to ΣN because the roles of K and \bar{K} and likewise of N and Ξ are interchanged. For convenience we summarize the isospin factors for the $\Xi\Sigma$ ($I = 3/2$) case in Table I. Those for $\Xi\Xi$ are identical to the ones for NN , with the replacement $N \leftrightarrow \Xi$ and $K \leftrightarrow \bar{K}$. The isospin factors for $\Sigma\Sigma$ and $I = 2$ are given in Table II. Note that the isospin factors for the one-pseudoscalar-meson exchange can be found in Table 3 of Ref. [23] (for $\Xi\Sigma$) and in Table 3 of Ref. [22] (for $\Sigma\Sigma$).

The explicit SU(3) symmetry breaking in the decay constants is taken into account. The empirical values for these constants are [42]

$$\begin{aligned} f_\pi &= 92.4 \text{ MeV}, \\ f_\eta &= (1.19 \pm 0.01) f_\pi, \\ f_K &= (1.30 \pm 0.05) f_\pi. \end{aligned} \quad (\text{A1})$$

and we use the central values in our study. A somewhat smaller SU(3) symmetry breaking occurs also in the axial coupling constants, see [43–45] but also [46, 47]. These effects are not taken into account in the present study. But we take the larger value $g_A = 1.29$ instead of $g_A = 1.26$ in order to account for the Goldberger–Treiman discrepancy [30].

As discussed in Appendix A.1 of Ref. [24] the evaluation of the two-pseudoscalar-meson exchange gives also rise to a polynomial part. We assume here that those contributions only renormalize the LO and NLO contact terms and, therefore, they are not considered. Some of the terms omitted involve the masses of the pseudoscalar mesons and the SU(3) symmetry breaking generated by them is assumed to be absorbed by the SU(3) symmetry breaking contact terms C_1^X and C_2^X . In principle, there is also an SU(3) symmetry breaking due to differences in the baryon masses as discussed in Appendix B.2 of Ref. [24]. However, since we consider here only channels with the same baryons in the initial and final states, their effects are tiny and are not taken into account here.

-
- [1] P. Adlarson *et al.* [WASA-at-COSY Collaboration], Phys. Rev. Lett. **112** (2014) 202311.
 - [2] A. Gal, in *From Nuclei to Stars, Festschrift in Honor of Gerald E Brown*, S. Lee (Ed.), World Scientific, Singapore 2011, p. 157, arXiv:1011.6322 [nucl-th].

- [3] R. L. Jaffe, Phys. Rev. Lett. **38**, 195 (1977) [Erratum-ibid. **38**, 617 (1977)].
- [4] J. T. Goldman, K. Maltman, G. J. Stephenson, Jr., K. E. Schmidt and F. Wang, Phys. Rev. Lett. **59** (1987) 627.

TABLE I. Isospin factors \mathcal{I} for $\Xi\Sigma$ with $I = 3/2$ for planar box, crossed box, triangle, and football diagrams consecutively. $B_{il}B_{ir}$ indicates the two baryons in the intermediate state and $\pi\pi$ etc. the exchanged pair of mesons M_1M_2 for planar box and crossed box diagrams. In case of the triangle diagrams there is only a single baryon in the intermediate state. See Ref. [24] for details of notation.

	$\begin{array}{c} M_1 M_2 \\ B_{il} B_{ir} \end{array}$	$\pi\pi$	$\pi\eta$	$\eta\pi$	$\eta\eta$	πK	ηK	$\begin{array}{c} M_1 M_2 \\ B_{il} B_{ir} \end{array}$	$\overline{K}\pi$	$\overline{K}\eta$	$\overline{K}\overline{K}$
planar box	$\Xi\Sigma$	1	1	1	1	2	2	$\Sigma\Sigma$	2	2	4
crossed box	$\Xi\Sigma$	3	1	1	1	0	0	$\Sigma\Sigma$	3	2	0
	$\Xi\Xi$	0	0	0	0	2	2	ΣN	0	0	2
	$\Xi\Lambda$	2	0	0	0	0	0	$\Lambda\Lambda$	1	0	0
								ΛN	0	0	2
								$\Lambda\Sigma, \Sigma\Lambda$	-1	0	0
	$\begin{array}{c} M_1 M_2 \\ B_i \end{array}$	$\pi\pi$	πK	ηK	KK	$\begin{array}{c} M_1 M_2 \\ B_i \end{array}$	$\overline{K}\pi$	$\overline{K}\eta$	$\overline{K}\overline{K}$		
triangle right	Ξ	-8	-2	$-2\sqrt{3}$	0	Σ	4	$2\sqrt{3}$	2		
						Λ	-2	0	-2		
	$\begin{array}{c} M_1 M_2 \\ B_i \end{array}$	$\pi\pi$	$\pi\overline{K}$	$\eta\overline{K}$	$\overline{K}\overline{K}$	$\begin{array}{c} M_1 M_2 \\ B_i \end{array}$	$K\pi$	$K\eta$	KK		
triangle left	Σ	-2	4	$2\sqrt{3}$	0	Ξ	-2	$-2\sqrt{3}$	4		
	Λ	-2	-2	0	0						
	N	0	0	0	-8						
football		16	6	6	4		6	6	4		

TABLE II. Isospin factors \mathcal{I} for $\Sigma\Sigma$ with $I = 2$ for planar box, crossed box, triangle, and football diagrams consecutively. $B_{il}B_{ir}$ indicates the two baryons in the intermediate state and $\pi\pi$ etc. the exchanged pair of mesons M_1M_2 for planar box and crossed box diagrams. In case of the triangle diagrams there is only a single baryon in the intermediate state. See Ref. [24] for details of notation.

	$\begin{array}{c} M_1M_2 \\ B_{il}B_{ir} \end{array}$	$\pi\pi$	$\pi\eta$	$\eta\pi$	$\eta\eta$	$\begin{array}{c} M_1M_2 \\ B_{il}B_{ir} \end{array}$	KK	$\bar{K}\bar{K}$
planar box	$\Sigma\Sigma$	1	1	1	1			
crossed box	$\Sigma\Sigma$	2	1	1	1	NN	0	4
	$\Lambda\Lambda$	1	0	0	0	$\Xi\Xi$	4	0
	$\Lambda\Sigma, \Sigma\Lambda$	1	0	0	0			
triangle left and right	Σ	-4	0	0	0	N	0	-4
	Λ	-4	0	0	0	Ξ	-4	0
football		32	0	0	0		8	8

- [5] F. Etminan *et al.* [HAL QCD Collaboration], Nucl. Phys. A **928** (2014) 89.
 [6] Z. Y. Zhang, Y. W. Yu, C. R. Ching, T. H. Ho and Z. D. Lu, Phys. Rev. C **61** (2000) 065204.
 [7] H. Pang, J. Ping, F. Wang and J. T. Goldman, Phys.

- Rev. C **66** (2002) 025201.
 [8] M. I. Buchoff, T. C. Luu and J. Wasem, Phys. Rev. D **85** (2012) 094511.
 [9] M. Yamada [HAL QCD Collaboration], PoS LATTICE **2013** (2014) 232.

- [10] G. Miller, Chin. J. Phys. **51** (2013) 466, arXiv:nucl-th/0607006.
- [11] T. A. Rijken, V. G. J. Stoks, Y. Yamamoto, Phys. Rev. C **59** (1999) 21.
- [12] T. A. Rijken, M. M. Nagels and Y. Yamamoto, Prog. Theor. Phys. Suppl. **185** (2010) 14.
- [13] V. G. J. Stoks and T. A. Rijken, Phys. Rev. C **59** (1999) 3009.
- [14] T. A. Rijken, M. M. Nagels and Y. Yamamoto, Few Body Syst. **54** (2013) 801.
- [15] Y. Fujiwara, Y. Suzuki and C. Nakamoto, Prog. Part. Nucl. Phys. **58** (2007) 439.
- [16] A. Reuber, K. Holinde, H. C. Kim and J. Speth, Nucl. Phys. A **608** (1996) 243.
- [17] S. R. Beane *et al.* [NPLQCD Collaboration], Phys. Rev. D **85** (2012) 054511.
- [18] K. Sasaki [HAL QCD Collaboration], PoS LATTICE **2013** (2014) 233; Contribution to the *Sixth Asia-Pacific Conference on Few-Body Problems in Physics*, Hahndorf, Australia, April 7-11, 2014.
- [19] H. Polinder, J. Haidenbauer and U.-G. Meißner, Nucl. Phys. A **779** (2006) 244.
- [20] S. Weinberg, Phys. Lett. B **251** (1990) 288.
- [21] S. Weinberg, Nucl. Phys. B **363** (1991) 3.
- [22] H. Polinder, J. Haidenbauer and U.-G. Meißner, Phys. Lett. B **653** (2007) 29.
- [23] J. Haidenbauer and U.-G. Meißner, Phys. Lett. B **684** (2010) 275.
- [24] J. Haidenbauer, S. Petschauer, N. Kaiser, U.-G. Meißner, A. Nogga and W. Weise, Nucl. Phys. A **915** (2013) 24.
- [25] S. Petschauer and N. Kaiser, Nucl. Phys. A **916** (2013) 1.
- [26] J. Haidenbauer, U.-G. Meißner, A. Nogga and H. Polinder, Lect. Notes Phys. **724** (2007) 113.
- [27] J. J. de Swart, Rev. Mod. Phys. **35** (1963) 916.
- [28] C. B. Dover and H. Feshbach, Annals Phys. **198** (1990) 321.
- [29] C.M. Vincent and S.C. Phatak, Phys. Rev. C **10** (1974) 391.
- [30] E. Epelbaum, W. Glöckle and U.-G. Meißner, Nucl. Phys. A **747** (2005) 362.
- [31] E. Epelbaum, H. Krebs and U.-G. Meißner, arXiv:1412.0142 [nucl-th].
- [32] R. A. Arndt, W. J. Briscoe, I. I. Strakovsky and R. L. Workman, Phys. Rev. C **76** (2007) 025209.
- [33] SAID Partial-Wave Analysis Facility, <http://gwdac.phys.gwu.edu/>
- [34] B. Holzenkamp, K. Holinde and J. Speth, Nucl. Phys. A **500** (1989) 485.
- [35] J. Haidenbauer and U.-G. Meißner, Phys. Rev. C **72** (2005) 044005.
- [36] J. Nagata, H. Yoshino, V. Limkaisang, Y. Yoshino, M. Matsuda and T. Ueda, Phys. Rev. C **66** (2002) 061001.
- [37] J. Haidenbauer and U. G. Meißner, Phys. Lett. B **706** (2011) 100.
- [38] J. Haidenbauer and U. G. Meißner, Nucl. Phys. A **881** (2012) 44.
- [39] L. Adamczyk *et al.* [STAR Collaboration], arXiv:1408.4360 [nucl-ex].
- [40] J.K. Ahn *et al.*, http://j-parc.jp/researcher/Hadron/en/pac_1107/pdf/KEK_J-PARC-PAC2011-03.pdf
- [41] A. M. Gasparyan, J. Haidenbauer and C. Hanhart, Phys. Rev. C **85** (2012) 015204.
- [42] K. A. Olive *et al.* [Particle Data Group Collaboration], Chin. Phys. C **38** (2014) 090001.
- [43] P. G. Ratcliffe, Phys. Lett. B **365** (1996) 383.
- [44] T. Yamanishi, Phys. Rev. D **76** (2007) 014006.
- [45] J. F. Donoghue and B. R. Holstein, Phys. Rev. D **25** (1982) 2015.
- [46] V. Bernard, L. Elouadrhiri and U.-G. Meißner, J. Phys. G **28** (2002) R1.
- [47] I. J. General and S. R. Cotanch, Phys. Rev. C **69** (2004) 035202.